

Chapter 2

REVIEW OF FLUID AND PARTICLE MECHANICS

2.1 Introduction

Before considering the flow of mixtures of liquids and solid particles, we must first treat the flow of single-phase liquids and the motion of particles in liquids. These topics also provide an introduction to concepts, terminology and notation used in later chapters. The treatment in this chapter is at the level of a review, intended primarily to reinforce knowledge which readers will have encountered in their undergraduate engineering curriculum, but may have not utilized in the interim. As in other parts of this book, the level of presentation is directed to practical engineering application. This chapter is not intended as an introduction to fluid mechanics in general, to turbulence, or to the micromechanics of particle-fluid systems. All these subjects have significance for fundamental research, but they are not required for an engineering treatment of slurry flow.

To characterise a simple fluid such as water only two material properties are required: density and viscosity. The density, denoted by ρ , represents the mass of fluid per unit volume. The viscosity is a measure of the resistance of the fluid to deformation by shearing, and is best illustrated by reference to a conceptual experiment illustrated in Fig. 2.1. The fluid fills a gap of

thickness y between two flat parallel plates. The plate forming the $y = 0$ plane is kept stationary, while the other plate (at $y = Y$) is moved parallel to

the first at a steady velocity U . The fluid immediately in contact with each solid plate keeps the same velocity as the plate; this is known as the 'non-slip boundary condition'. Thus the velocity of the fluid at $y = 0$ is zero and at $y = Y$ is U . The fluid velocity, u , at any intermediate position is yU/Y . The quantity U/Y is the velocity gradient in the fluid, denoted by du/dy . Its significance is that it represents the rate of shear deformation of the fluid; it is therefore known as the 'rate of shear strain' or, more simply, the 'shear rate'.

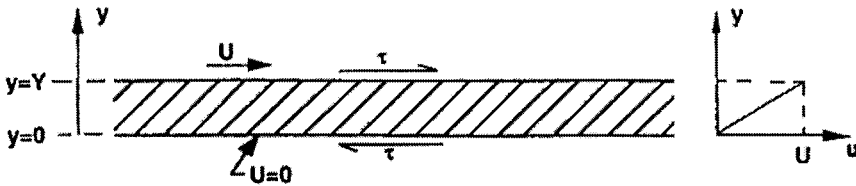


Figure 2.1. Shear deformation of a fluid (schematic)

To maintain the steady motion in Fig. 2.1, it is necessary to apply a force to the moving plate and an equal and opposite restraining force to the stationary plate. These forces are parallel to the plates, and in the direction of their relative motion. The force on one plate per unit area is known as the 'shear stress', denoted by τ . As shown in Fig. 2.1, it represents the shear stress exerted by each plate on the fluid in the gap. Simple Newtonian mechanics dictates that the fluid exerts an equal and opposite shear stress on the plate, and that the shear stress within the fluid at any plane parallel to the plates is also τ .

Conceptually, an experiment like that in Fig. 2.1 could be used to measure τ as a function of du/dy . In practice, flat plates are inconvenient; practicable ways to measure viscosity are introduced in Chapter 3. For a simple fluid like water, the relationship between τ and shear rate takes the form shown in Fig. 2.2, with τ linearly proportional to du/dy . This type of relationship defines a 'Newtonian fluid', and the constant of proportionality is known as the 'shear viscosity' (or simply the 'viscosity') and will be denoted by μ . Thus

$$\tau = \mu \frac{du}{dy} \quad (2.1)$$

Equation 2.1 is the ‘constitutive equation’ of a Newtonian fluid. The ratio μ/ρ is known as the ‘kinematic viscosity’ of the fluid, denoted by ν .

Values for the density and viscosity of water are given in Table 2.1. For practical purposes, over the range of conditions encountered in the industries using hydraulic transport, liquids are incompressible so that ρ and μ can be taken as independent of pressure. However they both depend on temperature. Specifically, the viscosity of water decreases significantly with increasing temperature.

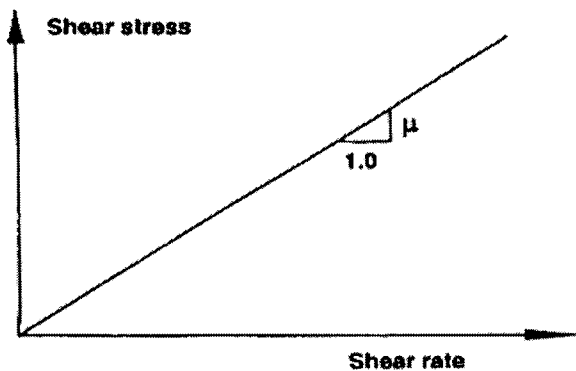


Figure 2.2. Characterisation of a Newtonian fluid (schematic)

Table 2.1. Properties of Water

Temperature (°C)	Density, ρ (kg/m ³)	Viscosity, $\mu \times 10^3$ (Pa.s)	Kinematic viscosity, $\nu \times 10^6$ (m ² /s)	Vapour pressure, p_v (kPa)
0	999.8	1.781	1.785	0.61
5	1000.0	1.518	1.519	0.87
10	999.7	1.307	1.306	1.23
15	999.1	1.139	1.139	1.70
20	998.2	1.002	1.003	2.34
25	997.0	0.890	0.893	3.17
30	995.7	0.798	0.800	4.24
40	992.2	0.653	0.658	7.38
50	988.0	0.547	0.553	12.33
60	983.2	0.466	0.474	19.92
70	977.8	0.404	0.413	31.16
80	971.8	0.354	0.364	47.34
90	965.3	0.315	0.326	70.10
100	958.4	0.282	0.294	101.33

2.2 Basic Relations for Flow of Simple Fluids

Much of this book is concerned with steady motion, in which the mean velocity at any point does not change with time (although it may vary with location). Whether the flow is steady or unsteady, analysis is based on three fundamental laws: the continuity balance (or conservation of matter); linear or angular momentum balances (which amount to the application of Newton's laws to fluids); and the mechanical energy balance (which is essentially the first law of thermodynamics applied to fluids). Some simple applications of these laws to solid-liquid mixtures are considered in Section 2.4. For steady flow of an incompressible fluid in a pipe or conduit, the continuity equation states simply that the volumetric flow is the same through each section across the pipe. Consider a pipe in which the diameter changes between sections A and B, as shown schematically in Fig. 2.3. If the total volumetric flowrate in the pipe is Q , and the pipe is taken to be 'running full', then the mean velocity at section A is

$$V_A = 4Q/\pi D_A^2 \quad (2.2)$$

where D_A is the internal pipe diameter at A, so that the pipe's cross-sectional area is $\pi D_A^2/4$. Similarly, at section B the mean velocity is

$$V_B = 4Q/\pi D_B^2 \quad (2.3)$$

The equation of continuity for this section of pipe then takes the form

$$Q = \pi D_A^2 V_A / 4 = \pi D_B^2 V_B / 4 \quad (2.4)$$

For cases in which it is necessary to consider the local velocity in the pipe at distance r from the axis, i.e. $u(r)$, then the total volumetric flow is evaluated from the integral

$$Q = \int_0^{D/2} u 2\pi r dr = 2\pi \int_0^{D/2} u r dr \quad (2.5)$$

in which the area of the element from r to $(r+dr)$ is $2\pi r dr$ and the velocity through it is u . Specific applications of Eq. 2.5 are considered below, and in Chapter 3.

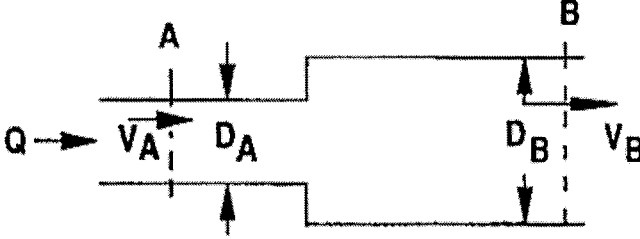


Figure 2.3. Flow in a pipe with change in diameter (schematic)

We next turn to the linear momentum equation, considering the simple case illustrated by Fig. 2.4: a fluid in steady motion through a straight horizontal pipe of constant diameter. Flow is 'fully developed', i.e. conditions do not vary between positions along the pipe. Therefore the shear stress exerted by the pipe walls on the fluid, τ_o , is the same at all sections. Between two sections A and B, a distance L apart, the total area of pipe wall is πDL so that the total force exerted by the pipe walls on the fluid is $\pi DL\tau_o$. The linear momentum equation applied to this case of steady uniform fully-developed flow states that the total force on the fluid between sections A and B must be zero, (because the momentum flux across section A is equal to that across section B), giving

$$\frac{\pi D^2}{4} (p_A - p_B) + \pi DL \tau_o = 0 \quad (2.6)$$

where p_A and p_B are the (static) pressures in the fluid at the two sections. Rearranging Eq. 2.6

$$-\frac{dp}{dL} = -\frac{(p_A - p_B)}{L} = \frac{4 \tau_o}{D} \quad (2.7)$$

or

$$\tau_o = - \frac{(p_A - p_B) D}{4L} \quad (2.8)$$

Equations 2.7 and 2.8 apply whether or not the fluid is Newtonian (i.e. obeys Eq. 2.1).

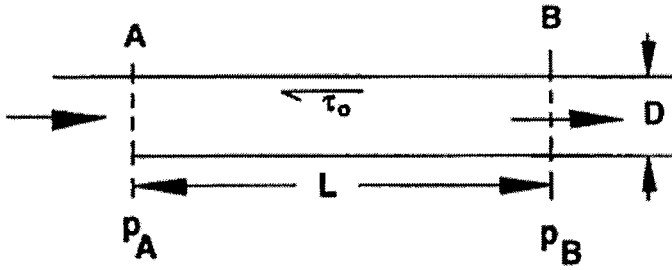


Figure 2.4. Flow in a straight horizontal pipe of constant diameter (schematic)

Another basic equation, for angular momentum, is needed for the analysis of centrifugal pumps. It will be presented in that context in Chapter 9. The energy equation is the next to be dealt with here. The mechanical energy balance for a flowing fluid is usually written in the form known as 'Bernoulli's equation'. It will be given here in terms of the 'head' of the fluid. 'Head' is a concept used extensively by Civil and Mining Engineers, and much of the literature on hydraulic conveying is written in terms of head and 'hydraulic gradient' (see below). Head is a measure of the mechanical energy of a flowing fluid per unit mass. It indicates the height by which the fluid would rise if the energy were converted to potential energy, and therefore has the units of length. The 'total dynamic head' of a fluid of density ρ flowing at velocity V in a pipe at elevation z above a reference level and at pressure p is

$$H = \frac{V^2}{2g} + \frac{p}{\rho g} + z \quad (2.9)$$

where the first term in this expression represents the kinetic energy of the fluid ('velocity head'), the second results from the static pressure in the fluid ('pressure head'), and the final term is the elevation ('static head').

Now consider a liquid propelled by a centrifugal pump, as shown in Fig. 2.5. Upstream of the pump, at section A on the pump suction, the total dynamic head of the fluid is H_A . Similarly, at section B on the pump

discharge, the total dynamic head is H_B . The increase in head across the pump, which is a simple measure of the energy imparted to the fluid by the pump, is known as the 'total developed head', TDH; i.e.

$$TDH = H_B - H_A = \frac{V_B^2 - V_A^2}{2g} + \frac{p_B - p_A}{\rho g} + (z_B - z_A) \quad (2.10)$$

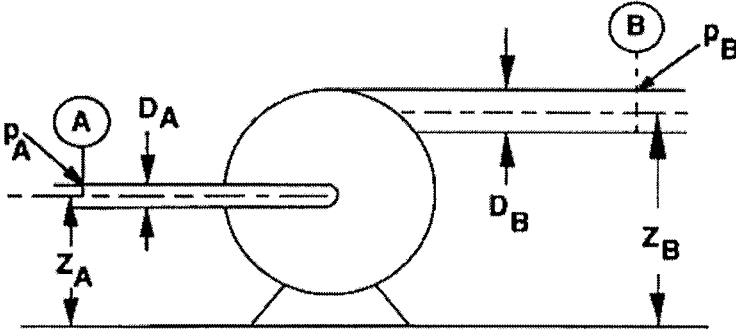


Figure 2.5. Fluid passing through a centrifugal pump (schematic)

In terms of the total volumetric flow rate, Q , and the pipe diameters at the two sections, D_A and D_B , (Eq. 2.2 and 2.3), the TDH equation becomes

$$TDH = \frac{8Q^2}{\pi^2 g} \left(\frac{1}{D_B^4} - \frac{1}{D_A^4} \right) + \frac{(p_B - p_A)}{\rho g} + (z_B - z_A) \quad (2.11)$$

The second term in Eq. 2.11, the 'pressure head', is normally by far the largest. The 'static head' term ($z_B - z_A$) is usually relatively small, and depends on the pump geometry and dimensions. Centrifugal pumps are sometimes made with different suction and discharge diameters (see Chapter 8), so that the first or 'velocity head' term can become significant at large flowrates.

For a fluid flowing in a straight horizontal pipe of constant diameter, the only head term which varies along the pipe is that arising from changes in pressure. For the flow shown in Fig. 2.4, the reduction in head per unit length of pipe is known as the 'hydraulic gradient':

$$i = - \frac{(P_A - P_B)}{\rho g L} = \frac{4 \tau_o}{\rho g D} \quad (2.12)$$

Here i has been related to the wall shear stress, τ_o , using Eq. 2.7. The units of the hydraulic gradient are (m head lost)/(m pipe run), or feet of head per foot of pipe. Thus the numerical value of i is independent of the system of units used. However, i is not strictly a dimensionless number: for example, if the flow took place on the moon or in any other environment of changed gravity, the value of i would be different even though τ_o and the pressure gradient were unchanged.

A simple illustration of the significance of i is given by Fig. 2.6. If we imagine that 'sight glasses' are attached to the pipe - i.e. vertical open-ended transparent tubes - then the height to which the fluid rises in each sight glass shows the pressure head inside the pipe at that point. For steady fully-developed pipe flow, with constant hydraulic gradient and pressure gradient, the levels in sight glasses set along the pipe will lie on a straight line. This is known as the 'hydraulic grade line', and its inclination is the hydraulic gradient, i .

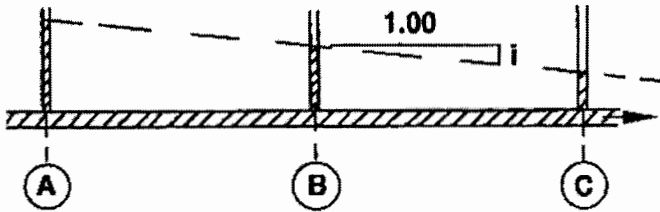


Figure 2.6. Significance of hydraulic gradient (schematic)

Consider now a pipe at an angle to the horizontal, as shown in Fig. 2.7. The pressure difference is measured between two sections, A and B, by connecting the pipe at these points to a manometer or a differential pressure sensor. Point B is Δz above A. The sensor is h above A, and therefore $(\Delta z - h)$ below B, and the connections from the sensor to the pipe are filled with the same fluid as in the pipe, of density ρ . If the pressure in the pipe at A is p_A , then the pressure on the upstream side of the sensor is lower by the hydrostatic column h :

$$p_A' = p_A - \rho g h \quad (2.13)$$

Similarly, the pressure on the other side of the sensor is

$$p_B' = p_B + \rho g(\Delta z - h) \quad (2.14)$$

Thus the pressure difference actually measured will be

$$\Delta p = p_A' - p_B' = p_A - (p_B + \rho g \Delta z) \quad (2.15)$$

i.e. the sensor will measure the change in the combination of pressure head and static head between A and B. For the case where the pipe is of constant section this is equal to the change in total head, i.e. $\rho g L$ where L is the distance from A to B. Thus a simple manometric measurement such as that illustrated in Fig. 2.7 serves to measure the hydraulic gradient.

Standard methods for predicting i for Newtonian fluids are given in the following Section. For slurry flow very careful definitions of hydraulic gradient are required. These will be introduced in Section 2.4.

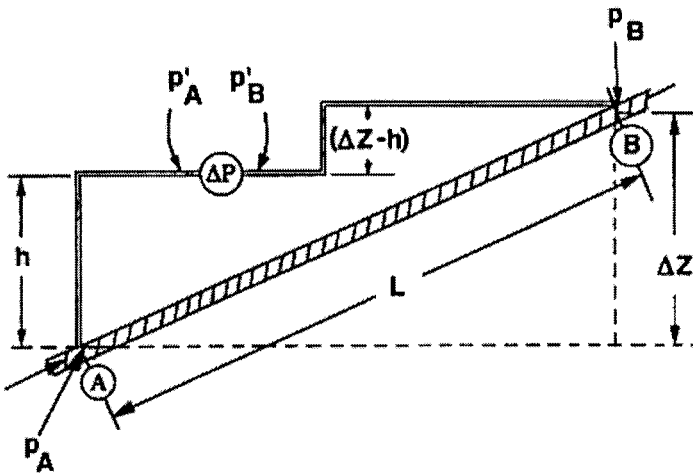


Figure 2.7. Measurement of hydraulic gradient in an inclined pipe (schematic)

2.3 Friction in Laminar and Turbulent Flow of Simple Fluids

Figure 2.8 shows a fluid flowing along a straight horizontal cylindrical pipe under the action of the pressure gradient dp/dx , where x is distance measured along the pipe. From Eq. 2.8, the shear stress at the pipe wall is

$$\tau_o = \frac{D}{4} \left(-\frac{dp}{dx} \right) \quad (2.16)$$

A similar force balance on the fluid within the cylinder of radius r coaxial with the pipe shows that the shear stress varies across the pipe section as shown in Fig. 2.8, and at radius r the shear stress is

$$\tau = \frac{r}{2} \left(-\frac{dp}{dx} \right) \quad (2.17)$$

It is now necessary to introduce an important distinction between two modes of flow of a fluid. In *laminar* flow, each element of the fluid moves on a steady path; in the case of flow in a pipe, all these paths are straight and parallel to the axis. In general, this type of motion occurs when viscous effects in the fluid predominate. In *turbulent* flow, elements of fluid follow irregular fluctuating paths caused by moving eddies. Thus, although the average or 'mean' velocity at any point within the fluid is parallel to the wall, the instantaneous velocity fluctuates in both magnitude and direction. In general, turbulent flow occurs when inertial effects predominate. For water in pipes of industrial scale, the flow is invariably turbulent. However, laminar flow can be important for non-settling slurries, which are discussed in Chapter 3.

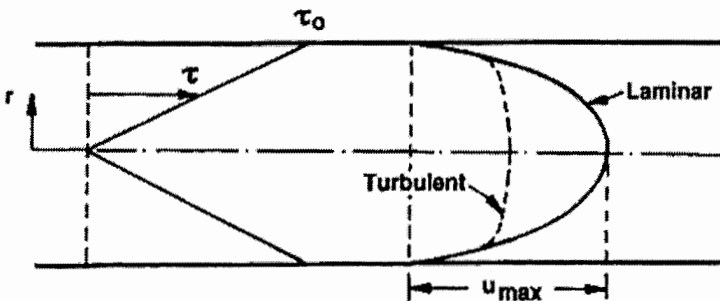


Figure 2.8. Stress and velocity distributions in pipe flow

Equation 2.17 applies whether the flow is laminar or turbulent. However, the resulting velocity profile in the pipe differs between the two types of flow. Consider first a Newtonian fluid in laminar flow, for which Eq. 2.1 applies in the form

$$\tau = \mu \left(-\frac{du}{dr} \right) \quad (2.18)$$

where u is the velocity at radius r . From Eq. 2.17 and 2.18,

$$\frac{du}{dr} = \frac{r}{2\mu} \left(\frac{dp}{dx} \right) \quad (2.19)$$

To obtain the velocity profile, Eq. 2.19 is integrated with the two conditions:

i. by symmetry, the velocity gradient is zero on the pipe axis, i.e. $du/dr = 0$ at $r = 0$;

ii. from the no-slip condition, the velocity is zero at the wall, i.e. $u = 0$ at $r = D/2$.

The resulting velocity profile takes the characteristic parabolic form, shown in Fig. 2.8 and given by

$$u = u_{\max} \left(1 - \frac{4r^2}{D^2} \right) \quad (2.20)$$

Fluids with other than Newtonian properties have slightly different velocity profiles, to be mentioned in Chapter 3. In Eq. 2.20, u_{\max} is the maximum velocity in the pipe, which occurs on the axis and is given by

$$u_{\max} = \frac{D \tau_o}{4\mu} = \frac{D^2}{16\mu} \left(-\frac{dp}{dx} \right) \quad (2.21)$$

Using Eq. 2.5, the total flowrate in the pipe is obtained as

$$Q = \frac{\pi D^2}{8} u_{\max} \quad (2.22)$$

Thus the mean velocity in the pipe, as defined in Eq. 2.2, is

$$V = 4Q/\pi D^2 = u_{\max}/2 \quad (2.23)$$

i.e. for a Newtonian fluid in laminar flow in a cylindrical pipe, the maximum velocity is twice the mean velocity. Finally, from Eq. 2.21 and 2.22

$$Q = \frac{\pi D^4}{128\mu} \left(-\frac{dp}{dx} \right) \quad (2.24)$$

and

$$\tau_o = \mu \left(\frac{8V}{D} \right) \quad (2.25)$$

Equation 2.25 will be generalised in Chapter 3 for non-Newtonian fluids.

If the fluid is in turbulent flow, Eq. 2.18 no longer applies, because the fluctuations exchange slow- and fast-moving fluid across surfaces within the flow. The effect of this momentum transfer is to set up stresses, known as 'Reynolds stresses', which dominate over the purely viscous stresses except near the walls. As a result, the velocity profile takes the form shown schematically in Fig. 2.8, rather flat in the central core of the flow but with a large velocity gradient in the wall region.

A basic parameter in turbulent flow is the group $\sqrt{\tau_o/\rho}$ which has the dimensions of velocity. It is known as the 'shear velocity' and is denoted by U_* . The velocity fluctuations associated with turbulent eddies have the same order of magnitude as the shear velocity. In fully turbulent flow the velocity gradient du/dy is directly proportional to U_* and inversely proportional to the 'mixing length'. This length is related to the size of the turbulent eddies, and for turbulent flow near a pipe wall the mixing length is evaluated as κy where y is the distance from the wall and κ is von Karman's coefficient. The value $\kappa = 0.4$ is often employed, and will be used here, giving the velocity gradient as $2.5U_*/y$.

The local velocity, u , obtained by integration, varies with the logarithm of y . If the pipe wall is 'hydraulically smooth', the velocity distribution is given by

$$\frac{u}{U_*} = 2.5 \ln \left[\frac{yU_*}{\nu} \right] + 5.5 \quad (2.26)$$

where \ln indicates the natural logarithm. The left hand side of this equation is a dimensionless velocity, denoted u^+ , while the ratio yU_*/ν is a dimensionless distance from the wall, denoted y^+ . At small values of y^+ the logarithmic velocity law of Eq. 2.26 will not apply, because immediately adjacent to a smooth wall there is a 'sub-layer' where viscous stresses are more important than Reynolds stresses and the flow can be considered to be laminar. As viscosity is dominant here, du/dy must equal τ_o/μ , by Eq. 2.1. This relation gives a linear variation of u with y , equivalent to the statement that u^+ equals y^+ at small values of y^+ .

This velocity relation extends from the smooth wall at $y^+=0$ out to about $y^+ = 5$ (see Fig. 2.9). Here turbulence first begins to be felt. The 'buffer layer' (from $y^+ = 5$ to a value of y^+ defined by various authors as between 25 and 50) is characterised by a gradual shift to fully turbulent flow, so that Eq. 2.26 becomes strictly valid only for y^+ greater than the buffer-layer limit. Additional information on velocity profiles may be found in Kay & Nedderman (1985) and Reynolds (1974). Although mathematical analysis of the buffer layer may be required in sophisticated treatments of turbulence, for most engineering purposes it is sufficient to employ a simplified treatment in which the transition to turbulent behaviour is assumed to occur abruptly at the point where Eq. 2.26 intersects the linear velocity relation applicable near the wall. At this point both y^+ and u^+ equal 11.6. In effect, the sub-layer is assumed to extend from the wall to $y^+ = 11.6$, and Eq. 2.26 is used for all larger values of y^+ . The thickness δ of this sub-layer (referred to as the viscous sub-layer) is given by

$$\delta = \frac{11.6 \mu}{(\rho_f \tau_o^{1/2})} = \frac{11.6 \mu}{\rho_f V} \left(\frac{8}{f} \right)^{1/2} \quad (2.27)$$

where f is the friction factor defined in Eq. 2.29 below. Thus the sub-layer becomes thinner as the flow in the pipe is increased.

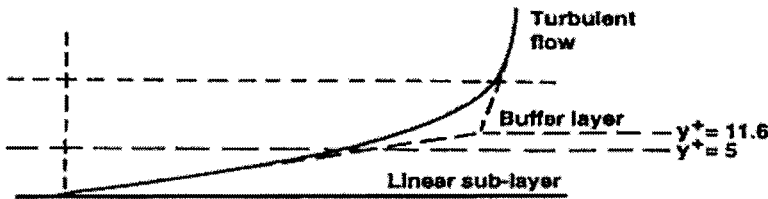


Figure 2.9. Velocity profile near wall in turbulent pipe flow

As the axis of the pipe is approached, the observed velocity profile diverges somewhat from the logarithmic law of Eq. 2.26. Detailed models of turbulent flow take this divergence into account, but for present purposes the logarithmic law is adequate for all of the flow except the viscous sub-layer. As this layer usually occupies a very small portion of the pipe area (See Example 2A, below), the average velocity V (the discharge divided by the section area $\pi D^2/4$) can be obtained by integrating Eq. 2.26. The result may be written

$$\frac{V}{U_*} = 2.5 \ln \left(\frac{U_* D}{\nu} \right) \quad (2.28)$$

Both dimensionless groups in this equation merit careful consideration. The ratio V/U_* can be expressed directly in terms of the dimensionless group known as the 'friction factor'. In this book we use the Moody form of the friction factor, defined as

$$f = 8 \tau_o / \rho V^2 \quad (2.29)$$

This is the definition commonly used by Civil and Mechanical engineers, whereas Chemical engineers may be more familiar with the Fanning friction factor, equal to $f/4$. From Eq. 2.29, it follows that $V/U_* = (8/f)^{1/2}$, or

$$U_* = V(f/8)^{1/2} \quad (2.30)$$

The dimensionless quantity $U_* D/\nu$ found in Eq. 2.28 is called the 'shear Reynolds number' Re_* which, like the better known 'pipe Reynolds number' Re (i.e. VD/ν), gives an indication of the state of flow. For cases where the pressure gradient, pipe diameter and fluid properties are known, U_* and Re_* can be determined immediately, and the mean velocity V is found by substituting these quantities into Eq. 2.28.

In cases where V and Re are known and U_* (and the pressure gradient) are required, use is made of the relation

$$Re_* = \frac{U_* D}{\nu} = \left(\frac{f}{8} \right)^{1/2} \frac{VD}{\nu} = Re \left(\frac{f}{8} \right)^{1/2} \quad (2.31)$$

On this basis Eq. 2.28 takes the form

$$(8/f)^{1/2} = 2.5 \ln(Re(f/8)^{1/2}) \quad (2.32)$$

With Re known, this equation can be solved for f . Although iteration is required, the range of f is small and the solution can be obtained quickly.

It should be noted that Eq. 2.32 (like Eq. 2.28, from which it is derived) applies only to turbulent flow with 'hydraulically smooth' pipe walls. This type of behaviour does not require asperities to be completely absent from the pipe wall, merely that the size, ε , of the typical roughness asperity is too small to penetrate the laminar sub layer and influence the turbulent portion of the flow. For larger values of ε the relative roughness, ε/D , is a significant parameter influencing pipe friction. For 'fully rough' pipes the viscous sub-layer is hidden between the asperities on the pipe wall, so that the roughness interacts directly with the turbulent flow. In this case viscosity is no longer important and the friction equation depends on $\ln(D/\varepsilon)$ instead of $\ln(Re)$. An appropriate transition function which incorporates both 'smooth' and 'rough' behaviour as limiting cases is given by the Colebrook-White equation. Rearranged somewhat (Streeter and Wylie, 1979) it may be expressed as

$$\frac{V}{U_*} = (8/f)^{1/2} = -2.43 \ln \left[\frac{\varepsilon/D}{3.7} + \frac{2.51}{Re(f)^{1/2}} \right] \quad (2.33)$$

Here the inverse of the von Karman coefficient is assigned the value of 2.43, not significantly different from the 2.5 used in other friction equations. As was the case for Eq. 2.28, if the pressure gradient is known (together with D , ε , and v) Eq. 2.33 allows the mean velocity to be calculated directly. If Re is known, together with ε/D , the equation can readily be iterated for f . The same result can be obtained directly from a graph of the relationship given by Eq. 2.33. This plot is often known as the 'Moody diagram' or the 'Stanton-Moody diagram'. The portion of the diagram that is of interest here is displayed on Fig. 2.10.

Various regions can be distinguished on the Moody diagram. For $Re < 2,000$, f is independent of roughness and is given by

$$f = 64/Re \quad (2.34)$$

This range corresponds to laminar flow, and Eq. 2.34 is simply Eq. 2.25 written in terms of the dimensionless groups introduced above.

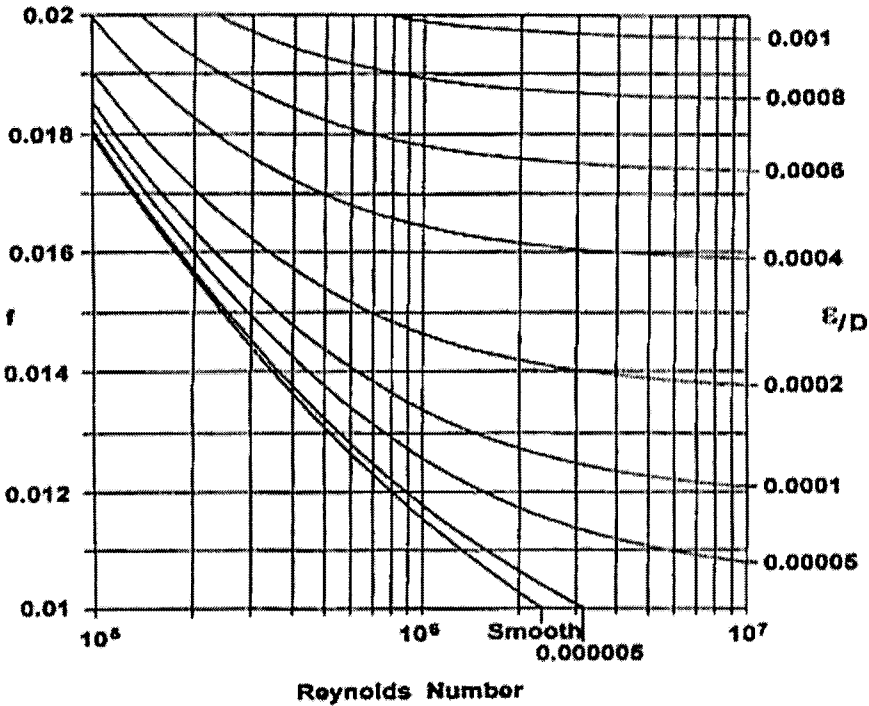


Figure 2.10. Pipe friction factor in normal operating range

For Re between about 2,000 and 3,000, flow can be laminar or turbulent; in industrial practice, it will almost always be turbulent. For $Re > 3,000$, flow is turbulent and f depends on both Re and ϵ/D : the curves on Fig. 2.10 are each drawn for one value of the relative roughness. In general, the friction factor decreases as Re increases and as roughness decreases. However, for sufficiently large values of Re , the laminar sub-layer becomes thinner than the asperities so that the range indicated as 'fully rough' is entered: the horizontal curves show that f now depends on ϵ/D but is independent of Re . Even in the 'transitional rough' range, the dependence of f on Re is weak. Thus, for turbulent flow in a given pipe with fixed relative roughness, it is frequently sufficient to treat the friction factor as a constant, characteristic of the pipe.

Detailed characterisation of roughness is a subject in itself, because the microscopic geometry will differ from one rough surface to another. However, commercial pipes are commonly characterised in terms of the 'equivalent sand-grain roughness'; i.e. their friction characteristics are compared with systematic measurements obtained by Nikuradse (1933) by

gluing sand grains to the walls of test sections of pipes. For example, the equivalent sand-grain roughness for commercial steel pipe is about 46 μm . It must be remembered that the effective roughness can change in service: corrosion can increase ε , while the polishing action of the particles in a slurry can reduce ε (and possibly also increase D if erosion is severe).

For a given flow of a given fluid in a given pipe, it is possible to calculate Re and ε/D , and hence obtain f from Fig. 2.10 or Eq. 2.33. From Eq. 2.12 and Eq. 2.29, the hydraulic friction gradient follows as

$$i = f \frac{V^2}{2gD} \quad (2.35)$$

As f is approximately constant for turbulent flow in a given pipe, Eq. 2.35 shows that the hydraulic gradient varies roughly as V^2 (or as Q^2).

The approach to estimating hydraulic gradient i summarised above and used throughout this book gives results essentially equivalent to those of other, more obviously empirical methods. An example of such methods is the 'C-factor' of Hazen and Williams which is still sometimes used in the mining industry. However, the use of f , with its dependence on Reynolds number and relative roughness, is preferred because it gives an indication of flow conditions and is more readily extended to interpretation of slurry flows.

For turbulent flow only, the loss of head associated with fittings such as bends and valves is usually estimated by multiplying the velocity head by a loss coefficient. The most widely-used loss coefficients are 0.5 for a standard 90-degree elbow (0.2 for a long-radius elbow) and 0.8 for an abrupt (unrounded) entry. At a pipe exit the full velocity head is lost, equivalent to an exit loss coefficient of 1.0. Further information on fitting losses is given in the McGraw-Hill Pump Handbook (Karassik et al., 2001).

The energy or head loss per unit length of pipe provides a measure of the hydraulic power required to deliver a flowrate Q through a horizontal pipe of length L , i.e.

$$P = \rho g Q i L \quad (2.36)$$

which can be rearranged, using Eq. 2.2 and 2.35, as

$$P = \frac{8\rho Q^3 f}{\pi^2 D^5} L \quad (2.37)$$

The very strong dependence on pipe diameter is worth noting. If power consumption is a major consideration, the economic incentive is towards using pipes of large diameter. The effect of this consideration on slurry system design will be evaluated in later chapters.

Example 2.A - Flow of Water in a Pipe

Water at room temperature of 20°C flows at 0.12 m³/s through a standard 8-inch steel pipe. Calculate:

- (a) the mean velocity and pipe Reynolds number;
- (b) the Moody friction factor;
- (c) the hydraulic gradient;
- (d) the thickness of the sub-layer;
- (e) the shear velocity
- (f) the hydraulic power required.

(a) Standard 'schedule 20' 8-inch pipe has an internal diameter of 0.2064 m. Therefore the pipe cross-sectional area is

$$\pi \times (0.2064)^2 / 4 = 0.03346 \text{ m}^2$$

and so the mean velocity V is

$$0.12 / 0.03346 = 3.59 \text{ m/s}$$

This mean velocity is towards the low end of the range typically used for settling slurries. For water at 20°C, $\rho = 998.2 \text{ kg/m}^3$ and $\mu = 1.002 \times 10^{-3} \text{ Pa.s}$ (Table 2.1). Therefore the Reynolds number is

$$Re = \frac{\rho V D}{\mu} = \frac{998.2 (3.59) (0.2064)}{1.002 \times 10^{-3}} = 7.38 \times 10^5$$

Because Re is dimensionless, the same value is obtained whatever system of units is used. Note that Re is high and the flow is well into the turbulent range.

(b) For commercial steel pipe, the equivalent sand-grain roughness is typically $4.6 \times 10^{-5} \text{ m}$, as noted previously. Therefore the relative roughness is

$$\varepsilon/D = 4.6 \times 10^{-5} / 0.2064 = 2.23 \times 10^{-4} = 0.000223$$

Referring to Fig. 2.10, flow conditions are in the 'transitional rough' range where the friction factor depends on the relative roughness and (weakly) on Re. From Fig. 2.10 or Eq. 2.33

$$f = 0.0152$$

Values for the Moody friction factor in the range 0.01 to 0.02 will prove to be fairly typical for water alone pumped at conditions commonly used for settling slurries.

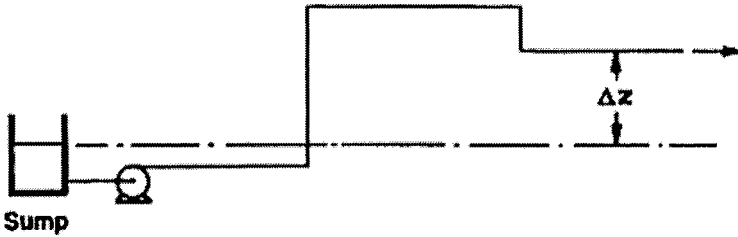


Figure 2.11. Simple piping system

(c) From Eq. 2.35, the hydraulic gradient is

$$i = \frac{f V^2}{2gD} = \frac{0.0152(3.59)^2}{2(9.81)(0.2064)} = 4.84 \times 10^{-2} \text{ m. head per m. pipe}$$

Values of the order of a few metres head per hundred metres of pipe are again typical of water pumped at conditions appropriate for a settling slurry.

(d) From Eq. 2.29, the wall shear stress is

$$\tau_o = \rho f V^2 / 8 = 998.2 (3.59)^2 (0.0152) / 8 = 24.4 \text{ Nm}^{-2}$$

The thickness of the viscous sublayer is estimated from Eq. 2.27 as

$$11.6 \mu / (\rho \tau_o)^{1/2} = 11.6 (1.002 \times 10^{-3}) / (998.2 \times 24.4)^{1/2} = 7.4 \times 10^{-5} \text{ m}$$

This value, i.e. 74 μm , can be compared with the equivalent sand-grain roughness, of 46 μm . As expected for a flow well into the 'transitional rough' range, the sub-layer thickness and the equivalent roughness are of comparable magnitude. The value for sub-layer thickness, a few tens of microns, is typical and is worth noting.

(e) From Eq. 2.30, the shear velocity is

$$U_* = V_m (f/8)^{1/2} = 3.59(0.0152/8)^{1/2} = 0.16 \text{ m/s}$$

and

$$U_* / V = (f/8)^{1/2} = 0.044$$

This value of U_* , of the order of $V/20$, is typical.

(f) The power required from the pumps is given by Eq. 2.37 as

$$\frac{P}{L} = \frac{8\rho Q^3 f}{\pi^2 D^5} = \frac{8(998.2)(0.12)^3(0.0152)}{\pi^2(0.2064)^5} = 57 \text{ W/m}$$

i.e. 57 kW/km, which again gives a typical order of magnitude for water alone.

In later chapters, we will examine the operability of piping systems using centrifugal pumps, by matching the 'system characteristic' with the 'pump characteristic'. Figures 2.11 and 2.12 illustrate this idea for a system conveying a liquid alone. For a simple piping system shown schematically in Fig. 2.11, the total head required varies with flowrate as shown by curve 1 in Fig. 2.12. The 'static lift' term, Δz , from the surface in the sump to the pipe discharge, does not depend on flow rate. The flow-dependent terms include the friction losses in the pipe and fittings, and also the 'velocity head' at the pipe discharge because this is not recovered as pressure. Thus, for a pump with head-discharge characteristic (see Chapter 9) given by curve 2, the system will operate at the discharge corresponding to the intersection of the characteristics at point A. Operation is stable, because the pump characteristic is falling while the system characteristic is rising. Thus a slight decrease in flow reduces the head demand of the system but increases the head delivered by the pump, to return operation to point A. Similarly, increases in flow are automatically returned to A. Closing a valve, for

example on the pump discharge, reduces the flow by increasing the resistance of the system, for example by moving the system characteristic to curve 3, so that the operating point moves to B. However, for a simple liquid with a rising system characteristic, operation remains stable.

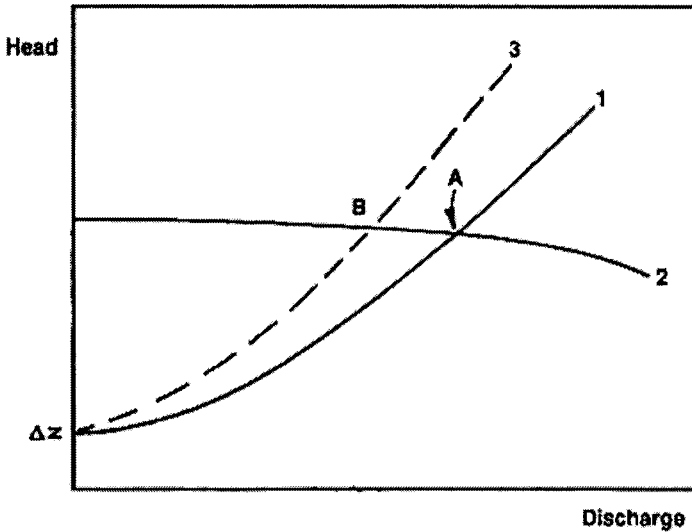


Figure 2.12. System and pump characteristics

2.4 Basic Relations for Slurry Flow

When we turn from flow of a simple liquid to that of a slurry, i.e. a mixture of solid particles in a carrier fluid, the need immediately arises for a more precise system of nomenclature. For example, instead of a single density, ρ , several densities must now be distinguished. These include the density of the fluid, ρ_f , that of the solid particles, ρ_s , and that of the mixture ρ_m . For a very large number of slurries, the carrier fluid is water, with density of approximately 1000 kg/m^3 . The symbol ρ_w is employed in this instance, using ρ_f for fluids of other densities. The value of ρ_w forms the basis for expressing the relative density or 'specific gravity' of other materials. For example there is a wide range of applications when the solids being conveyed have a density around 2650 kg/m^3 , a typical value for sand, and in this case the relative density, S_s or ρ_s/ρ_w , is 2.65. Although in many cases the fluid is standard-density water, this is not always the case. For example in marine dredging operations, the carrier fluid is sea water, for

which the relative density, denoted S_f , varies from place to place but has a typical value of about 1.03.

For a mixture of solids and fluid, the relative density S_m (i.e. the mean specific gravity of the mixture) is given by the general formula

$$S_m = S_f + (S_s - S_f) C_v \quad (2.38)$$

where C_v is the volumetric concentration, i.e. the fraction of the mixture volume which is occupied by the solids. When the fluid is water of standard density, S_f is unity and the equation for S_m becomes

$$S_m = 1 + (S_s - 1) C_v \quad (2.39)$$

The volumetric concentration, C_v , is employed in this book, but it should be noted that a different measure, the weight concentration C_w , is commonly used in some industries. If the weight concentration C_w is known, C_v can be calculated from: $S_f C_w / [S_s - (S_s - S_f) C_w]$. Conversely, C_w is given by the expression $S_s C_v / [S_f + (S_s - S_f) C_v]$. As we are concerned here with general approaches applicable to any slurry, we will work throughout in terms of *volume* concentration. This parameter provides a much clearer indication of slurry consistency, applicable whatever the solid density.

In specifying concentrations, care is required to distinguish between delivered and *in situ* values. The delivered concentration is the fraction of solids delivered from (or fed to) the conveying system. If the slurry discharged from the system is collected in a tank, then the volume fraction of solids for the mixture in this tank is the delivered volumetric concentration, denoted C_{vd} . On the other hand, the resident or *in situ* concentration is the average concentration present in the system, or in some part of it, such as a certain length of pipe. If, say, this length of pipe were isolated by suddenly closing valves at both ends (ignoring the effects of water-hammer), then the volumetric fraction of solids in the isolated pipe is the resident or *in situ* volumetric concentration, denoted C_{vi} .

Although it might appear at first sight that these two measures of concentration should give the same value, this is only the case for truly non-settling slurries for which there is no tendency for the two components to segregate. The values of C_{vd} and C_{vi} differ when the average velocity of the solids (V_s) is not the same as that of the fluid (V_f), and this is typically the case in stratified flows (see Chapter 3). Although it is not necessary to have stationary solids in the pipe for C_{vd} and C_{vi} to differ, an extreme example is

given by the case where a deposit of stationary solids fills, say, the lower half of the pipe. Water flows through the upper part of the pipe, but moves only a few solid particles, which tend to roll along the top of the bed. The *in situ* concentration C_{vi} is quite large, but as most of the solids are not moving at all, the *average* velocity of the solids is small, much less than that of the water. As a result, in this case the concentration of solids in the delivered mixture, C_{vd} , is much smaller than C_{vi} .

The volumetric flowrate of liquid, Q_f , is the product of V_f and the cross-sectional area occupied by the fluid, i.e. $(1-C_{vi})\pi D^2/4$. Similarly, the volumetric flowrate of solids is $V_s C_{vi} \pi D^2/4$. The total flowrate of the mixture, Q_m , is given by the sum of the fluid and solids flowrates, and is also equal to $\pi D^2/4$ times the mean velocity of the mixture. Thus

$$\frac{4 Q_m}{\pi D^2} = V_m = V_f (1 - C_{vi}) + V_s C_{vi} \quad (2.40)$$

The delivered volumetric concentration, C_{vd} , represents Q_s/Q_m , i.e.

$$C_{vd} = \frac{Q_s}{Q_m} = \frac{V_s}{V_m} C_{vi} \quad (2.41)$$

Equation 2.41 shows directly that the delivered concentration must be less than the *in situ* value provided V_s is less than V_m . This condition is described as 'lag', 'hold up' (or, less accurately, 'slip') of the solids. The 'lag' or 'slip' is the velocity difference $V_m - V_s$, and the lag ratio Λ is obtained by dividing this quantity by the mean velocity, i.e.

$$\Lambda = \frac{V_m - V_s}{V_m} \quad (2.42)$$

On this basis Eq. 2.42 is re-written

$$C_{vi} = \frac{1}{1 - \Lambda} C_{vd} \quad (2.43)$$

Thus, when there is hold-up of the solids relative to the liquid the *in situ* concentration is greater than the delivered concentration, and the difference between the two concentrations increases when the lag ratio increases.

This conclusion has a number of far-reaching implications. An obvious corollary is that measuring the *in situ* solids concentration, for example by a radiation technique (see Chapter 12), does not indicate the delivered concentration. A further corollary concerns the analysis of the transport of settling slurries, for which the hold-up effect is significant. As will be seen, the *in situ* concentration is most important in determining friction losses. However, design methods must be based on the delivered concentration, with the *in situ* concentration either inferred or not estimated explicitly. Furthermore, slurry testing must normally use closed-loop systems in which the inventory and therefore the resident concentration is fixed, and thus the delivered concentration will vary as V_m is changed. Hence the simple approach suitable for single-phase fluids cannot be applied to slurries.

Another area in which slurries require a more careful treatment than single-phase fluids is that of the friction gradient or energy gradient. In the form of the pressure gradient dp/dx , the friction loss associated with the flow of a slurry in a pipe is unambiguous. However, the expression of pressure loss as a 'hydraulic gradient' (such as m water per m length of pipe) is so common in slurry pipelining that it cannot be avoided. Only precise definitions of all quantities will prevent ambiguity. As expressed in Eq. 2.12, for a single fluid the hydraulic gradient is $(-dp/dx)/\rho g$. The possible ambiguity arises from the density to be used in this expression. For flows of water alone the appropriate density is ρ_w (approximately 1000 kg/m³), so that the corresponding hydraulic gradient is

$$i = \frac{l}{\rho_w g} \left(-\frac{dp}{dx} \right) \quad (2.44)$$

giving the friction loss as metres head of water per metre of pipe.

Following a proposal made by Dr. M.R. Carstens in the early years of the GIW Slurry Course, the symbol i is used in this book to denote 'hydraulic gradients' given by Eq. 2.44 and expressed in height of clear water per length of pipe. As both ρ_w and g are constants, this definition is equivalent to stating that, for a horizontal pipe, i is simply the pressure gradient divided by a constant (9810 N/m³ in S.I. units). The set of subscripts introduced above in connection with densities will also be employed here. Thus i_m represents the pressure gradient for a mixture, but expressed in height of water per length of line. Similarly i_f expresses the pressure gradient for a fluid (if different from water) in terms of height of water, and i_w applies when the fluid is water. (The similarity to the use of water as a reference fluid for specific gravity will be readily apparent.) In

evaluating the extra friction loss caused by the conveyed solids, we use the 'solids effect' ($i_m - i_f$), where i_f is the friction gradient for carrier liquid alone at flowrate equal to the mixture flowrate Q_m . The evaluation of this quantity will be discussed extensively in Chapters 4, 5 and 6.

An alternative definition of the mixture hydraulic gradient is based on the mean density of the delivered slurry, ρ_{md} (and the associated relative density S_{md}). For clarity, this will be noted by j rather than i , giving

$$j_m = \frac{l}{\rho_{md} g} \left(-\frac{dp}{dx} \right) = \frac{l}{S_{md} \rho_w g} \left(-\frac{dp}{dx} \right) \quad (2.45)$$

This measure of the hydraulic gradient is more useful for some purposes, such as matching system and pump characteristics (see Chapter 13). From Eq. 2.44 and 2.45, the two are related by

$$i_m = S_{md} j_m \quad (2.46)$$

Under some circumstances, to be examined in later chapters, it can happen that the additional pressure gradient attributable to the solids is proportional to the increase in slurry density, i.e. the 'equivalent fluid' model applies with

$$i_m = S_{md} i_w \quad \text{and} \quad j_m = i_w \quad (2.47)$$

A slurry of this type will be termed an 'equivalent fluid' because, in effect, it behaves as a single-phase liquid with the density of the delivered slurry.

2.5 Settling of Solids in Liquids

The properties of slurries depend very strongly on the tendency of the particles to settle out from the conveying liquid. For transport of settling slurries, an important parameter is the *terminal velocity*, v_t , i.e. the velocity at which a single particle settles through a large volume of quiescent liquid. The terminal velocity depends on the liquid properties (ρ_f and μ) on the particle diameter (d) and its density (ρ_s) and, to a lesser extent, on its shape. For vertical flow of settling slurries the *hindered settling velocity* is also of importance. When particles have fully settled, their concentration, achieved without compacting or vibrating the sediment, is referred to in later chapters as the 'loose packed' volume fraction, denoted C_{vb} .

Particle sizes are commonly reported as 'screen size', i.e. the opening in a standard sieve or screen. Particle size distributions are then reported as the fraction (by mass or weight) passing through one screen in the series but retained on the next. Standard screen series have often been expressed as 'mesh size' based on the number of openings per inch, but openings in mm (or μm) are now in common use.

In general, particles in slurries are not spherical, but the sphere represents a convenient reference case in the analysis. Figure 2.13 shows the forces acting on a rigid sphere settling through a fluid. The weight of the particle is partially reduced by the buoyancy of the surrounding fluid. When the spherical particle is moving steadily at its terminal velocity v_{ts} , the resulting 'immersed weight', 'submerged weight' or 'net weight' is balanced by the drag of the fluid:

$$F_D = \frac{\pi d^3}{6} (\rho_s - \rho_f) g \quad (2.48)$$

Calculation of the terminal velocity therefore depends on estimating the velocity at which Eq. 2.48 is satisfied. Since there is no general theoretical result which enables this equation to be solved for v_{ts} , we resort to dimensional analysis. In general, with f_n denoting some function,

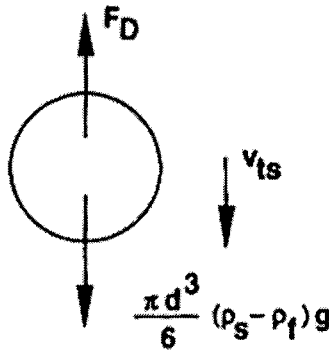


Figure 2.13. Single spherical particle falling at its terminal velocity

$$F_D \equiv fn(\rho_f, \mu, d, v_{ts}) \quad (2.49)$$

where v_{ts} refers specifically to the terminal velocity of a spherical particle. Given that there are five parameters and the usual three basic dimensions of mass, length and time, Buckingham's theorem shows that two dimensionless groups suffice to express Eq. 2.49 in general form. Most commonly, the two dimensionless groups selected are:

$$\text{drag coefficient : } C_D = \frac{8 F_D}{\pi d^2 v_{ts}^2 \rho_f} \quad (2.50)$$

$$\text{particle Reynolds number : } Re_p = \rho_f v_{ts} d / \mu \quad (2.51)$$

so that Eq. 2.49 is written in general form as

$$C_D \equiv fn(Re_p) \quad (2.52)$$

The function indicated in this equation has been fitted to the many determinations of drag or terminal velocity, to give the 'standard drag curve' shown in Fig. 2.14. For $Re_p < 3 \times 10^5$, which amply covers the range encountered in slurries, the curve is approximated well by an expression given by Turton & Levenspiel (1986)

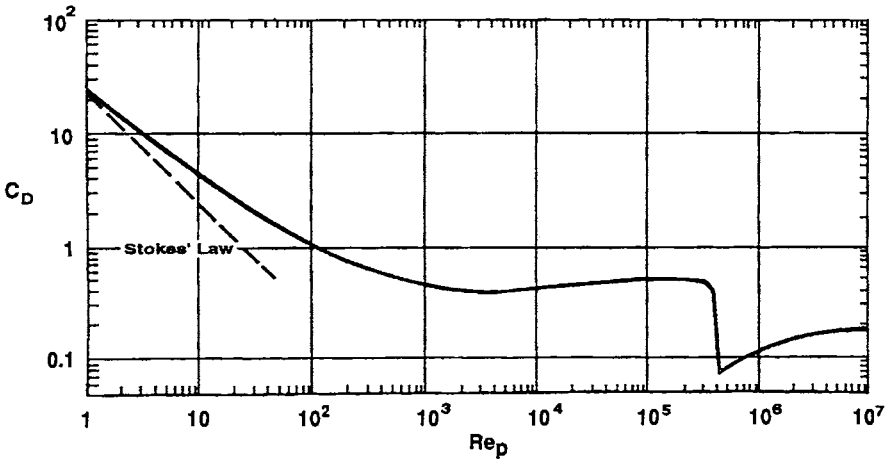


Figure 2.14. Standard drag coefficient curve for spheres

$$C_D = \frac{24}{Re_p} (1 + 0.173 Re_p^{0.657}) + \frac{0.413}{1 + 1.63 \times 10^4 Re_p^{-1.09}} \quad (2.53)$$

The terminal velocity can then be determined from Eq. 2.48 and 2.53, but the procedure is iterative, with successive estimates for v_{ts} updated to converge on the solution.

The reasons for the form of the curve in Fig. 2.14 are discussed in detail by Clift *et al.* (1978). For low particle Reynolds numbers, say $Re_p < 0.1$, Stokes' law applies, with the drag force given by the theoretical result:

$$F_D = 3 \pi \mu v_{ts} d \quad (2.54)$$

The terminal velocity follows as

$$v_{ts} = \frac{d^2 (\rho_s - \rho_f) g}{18 \mu} \quad (2.55)$$

At much larger Reynolds numbers, in the approximate range $750 < Re < 3 \times 10^5$, the drag coefficient is roughly constant and close to 0.445. This is known as the 'Newton's law' range, based on Newton's experiments with falling objects (e.g. inflated pigs' bladders falling within the dome of St. Paul's cathedral, see Newton, 1726). In this range the terminal velocity of a sphere falling through water can be calculated using

$$v_{ts} = 1.73 \sqrt{gd (S_s - 1)} \quad (2.56)$$

As a general guide for sand-density particles in water, Stokes' law applies for particles smaller than about $50 \mu\text{m}$, while Newton's law applies for particles larger than about 2mm .

As noted above, two independent dimensionless groups are needed to express empirical drag results in general form. However, these groups can be selected for convenience. Various possibilities and their uses are reviewed by Clift *et al.* (1978). Following the suggestion of Grace (1986), it is found convenient to define a dimensionless particle diameter d^* (equal to the cube root of what is often called the Archimides number)

$$d^* = [3 C_D Re_p^2 / 4]^{1/3} = d \left[\frac{\rho_f (\rho_s - \rho_f) g}{\mu^2} \right]^{1/3} \quad (2.57)$$

and a dimensionless terminal velocity

$$v_{ts}^* = Re_p / d^* = \left[\frac{4 Re_p}{3 C_D} \right]^{1/3} = v_{ts} \left[\frac{\rho_f^2}{\mu (\rho_s - \rho_f) g} \right]^{1/3} \quad (2.58)$$

so that Eq. 2.49 becomes in general dimensionless form

$$v_{ts}^* = fn(d^*) \quad (2.59)$$

and calculation of v_{ts}^* , and hence v_{ts} , requires no iteration. This functional relation has been worked out in considerable detail, and is entirely suitable for particles falling in Newtonian fluids. However, for the analogous case in non-Newtonian fluids (dealt with in Chapter 7) difficulties arise because the viscosity is included in both dimensionless variables. To cover both Newtonian and non-Newtonian cases, an alternative method has been worked out, as described by Wilson *et al.* (2003) and Wilson & Horsley (2004). This method is based on a pair of dimensionless variables that employ concepts developed in the pipe-flow analysis of Prandtl (1933) and Colebrook (1939).

The method expresses the velocity ratio (mean velocity to shear velocity) as a function of the shear Reynolds number (based on shear velocity rather than mean velocity). In pipe flow the shear velocity V^* is the square root of the ratio of the shear stress at the pipe wall (uniform for a circular pipe) to the fluid density. The shear stress set up on the surface of a spherical particle is non-uniform, but the mean surficial shear stress, denoted $\bar{\tau}$, forms a useful basis for analysis. This stress is given by the submerged weight force divided by the surface area of the sphere, which is πd^2 , where d is the sphere diameter. The submerged weight force is the product of the sphere volume $\pi d^3/6$ and $(\rho_s - \rho_f)g$, where g is gravitational acceleration and ρ_s and ρ_f are the densities of the solid and fluid phases, respectively. Thus the mean surficial shear stress is given by

$$\bar{\tau} = (\rho_s - \rho_f) g d / 6 \quad (2.60)$$

For the falling-particle case, the shear velocity is based on $\bar{\tau}$. Thus

$$V^* = \sqrt{(\rho_s - \rho_f)gd / 6\rho_f} \quad (2.61)$$

or, with S denoting ρ_s/ρ_f

$$V^* = \sqrt{(S-1)gd / 6} \quad (2.62)$$

For pipe flow, the velocity ratio is the mean velocity divided by V^* ; and for falling particles the analogous ratio is based on the terminal fall velocity of the particle V_t , giving V_t/V^* as the velocity ratio. The shear Reynolds number Re^* has the form:

$$Re^* = \rho_f V^* d / \mu \quad (2.63)$$

Here d is the particle diameter (analogous to the pipe diameter for the pipe-flow case) and, for a Newtonian fluid, μ is the viscosity.

Next, it is appropriate to investigate the form of the settling curve for Newtonian fluids for the V_t/V^* and Re^* axes. In terms of these variables, the drag coefficient equals $8/[V_t/V^*]^2$ and the conventional Reynolds number Re equals the product of Re^* and V_t/V^* . For Re larger than about 1100 the drag coefficient can be taken as effectively constant at 0.445, equivalent to $V_t/V^*=4.24$ for $Re^*>260$. At the other end of the Reynolds number range, settling obeys Stokes law which can be expressed as $V_t/V^*=Re^*/3$. In the intermediate region, the coordinates of individual points on the C_D - Re curve can be transformed into V_t/V^* and Re^* values and plotted on the new curve, which is found to have the shape shown on Fig. 2.15.

In developing Fig. 2.15, a series of points on the C_D - Re curve were calculated using the equation of Turton & Levenspiel (1986). These points were then transformed to V_t/V^* and Re^* co-ordinates, and equations were fitted to the transformed points. For $Re^* \leq 10$, the fit equation is:

$$V_t/V^* = Re^* / [3(1 + 0.08 Re^{*1.2})] + 2.80 / [1 + 3.0(10^4)(Re^{*-3.2})] \quad (2.64)$$

In the range $10 < Re^* < 260$ a different fit equation is used, based on $x = \log(Re^*/10)$ and $y = \log(V_t/V^*)$. It is:

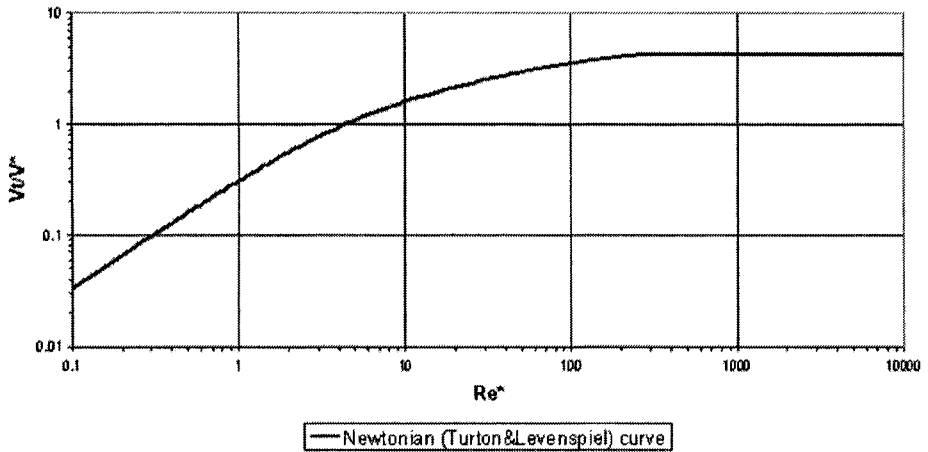


Figure 2.15. Curve of relative fall velocity versus shear Reynolds number (from Wilson *et al.*, 2003)

$$y = 0.2069 + 0.500 x - 0.158 x^{1.72} \quad (2.65)$$

The curve represented by these equations is shown, on logarithmic coordinates, on Fig. 2.15. As mentioned above, for $Re^* > 260$, $V_f/V^* = 4.24$.

Approaches to estimating terminal velocities for non-spherical particles have been reviewed by Clift *et al.* (1978). For the conditions of interest in hydraulic conveying, the most suitable approach is based on Heywood's 'volumetric shape factor'. In the range of particle Reynolds numbers from roughly unity to of order 100 - which is the range of interest here - a particle orients itself during settling so as to maximise the drag. Generally, this means that an oblate or lenticular particle, i.e. a shape with one dimension smaller than the other two, will settle with its maximum area horizontal. The drag of the fluid on the particle then depends most critically on this area, A_p . This is also the area seen if the particle lies in a stable position on a flat surface, for example a microscope slide. Therefore, for estimation of drag, the non-spherical particle is characterised by the 'area-equivalent diameter', i.e. the diameter of the sphere with the same projected area:

$$d_a = \sqrt{4 A_p / \pi} \quad (2.66)$$

For particles whose sizes are determined by sieving rather than microscopic analysis, d_a is slightly smaller than the mesh size. However, unless the

particles are needle-shaped, the difference between d_a and the screen opening is relatively small, generally less than 20%. The shape of the particle is described by the 'volumetric shape factor' defined as

$$K = (\text{volume of particle}) / d_a^3 \quad (2.67)$$

so that K is 0.524 for a sphere. Representative values for various mineral particle are given in Table 2.2. In general, the more angular or flakey the particle, the lower is the value of K .

Table 2.2. Typical values of volumetric shape factor for mineral particles

Mineral Particles	Typical K
Sand	0.26
Sillimanite	0.23
Bituminous coal	0.23
Blast furnace slag	0.19
Limestone	0.16
Talc	0.16
Plumbago	0.16
Gypsum	0.13
Flake graphite	0.023
Mica	0.003

The procedure for calculation of terminal velocity is first to use the method presented above to calculate v_{ts} for the sphere of diameter d_a and the same density as the particle of interest. The value for the non-spherical particle is then given by

$$v_t = \xi v_{ts} \quad (2.68)$$

where the velocity ratio ξ is a function of the shape factor, K , and a weak function of the dimensionless diameter d^* . Values for ξ are obtained from the curves in Fig. 2.16. It will be seen that, for common particles like sand and coal, the terminal velocity is typically 50-60% of the value for the equivalent sphere. The value of ξ allows for the lower volume (and therefore lower immersed weight) of the particle compared to the sphere, and also for differences in drag.

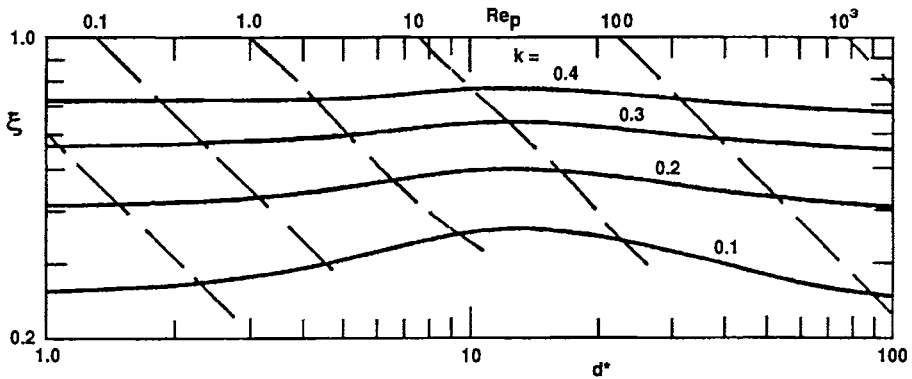


Figure 2.16. Ratio of terminal velocity of non-spherical particle to value for sphere, ξ , as function of dimensionless diameter, d^*

The hindered settling velocity, v_t' , is normally less than v_t and is strongly dependent on the volume concentration of solids. For fine particles in the 'clay' range, the hindered settling behaviour is dominated by the forces between the particles. These forces depend on the chemical nature of the particle surfaces and of the liquid, and specifically on acidity, electrolyte concentration, and trace concentrations of surface-active agents. At present, these effects cannot be predicted reliably. Exactly the same remarks apply to the rheological properties of slurries of these particles, and this leads to the need for the 'testing and scale-up' approach for non-settling slurries set out in Chapter 3. In general, the effect of interparticle forces reduces v_t' even more than purely hydrodynamic effects. However, if the particles flocculate or agglomerate, then the hindered settling velocity is increased.

For larger particles – those which behave as individual grains – the hindered settling velocity can be estimated reasonably reliably by the correlation of Richardson & Zaki (1954):

$$v_t' = v_t (1 - C_v)^n \quad (2.69)$$

Equation 2.69 allows for two phenomena which reduce v_t' below v_t : the increased drag caused by the proximity of other particles, and the upflow of liquid as it is displaced by the descending particles. The index n depends on d^* , and is larger for particles settling in the range of Stokes' law ($n = 4.6$) and smaller in the range of Newton's law ($n = 2.4$).

Example 2.B - Calculation of Terminal and Hindered Settling Velocities

Estimate the terminal velocity and hindered settling velocities of sand particles with shape factor 0.26 in water at room temperature. Consider particles of sizes 0.2, 0.5, 1.0 and 2.0 mm. (It will be shown in Chapter 6 that particle settling is of greatest significance for heterogeneous flow, which applies to particles in this size range.)

(a) Terminal Velocities of Equivalent Spheres.

For water at 20°C, $\rho_w = 998.2 \text{ kg/m}^3$ and $\mu = 1.002 \times 10^{-3} \text{ Pa.s}$ (from Table 2.1). The density of quartz sand is typically 2650 kg/m^3 . Therefore the shear velocity based on the mean surficial shear stress (Eq. 2.62) is:

$$V^* = \sqrt{(S_s - 1)gd} \text{ or } \sqrt{(1.65)9.81d}$$

with d in metres. Table 2.3 shows the values that were obtained for this quantity for the various particle sizes. Also shown in the table are values of Re^* , i.e. $\rho_f V^* d / \mu$. This quantity is used to calculate v_{ts}/V^* , using Eq. 2.64 for the 0.2 mm particle (for which $Re^* < 10$) and Eq. 2.65 for the other particles, based on their shear Reynolds numbers. Multiplying the ratio v_{ts}/V^* by V^* gives the fall velocity for a spherical particle, v_{ts} , which is shown in Table 2.3. Note that the 0.2 mm particles lie well beyond the Stokes' law range, while the 2 mm particles are not quite into the Newton's law range.

(b) Terminal Velocities of Sand Grains

To obtain the terminal fall velocity of the sand particles, the values of v_{ts} must be multiplied by the velocity ratio ξ , which, in turn, depends on the dimensionless particle size d^* , given by Eq. 2.57

$$d^* = \left[\frac{\rho_f (\rho_s - \rho_f) g}{\mu^2} \right]^{1/3} d$$

or

$$d^* = \left[\frac{998.2 (2650 - 998.2) (9.81)}{(1.002 \times 10^{-3})^2} \right]^{1/3} d = 2.526 \times 10^{+4} d$$

The values of the velocity ratio, ξ , are obtained from Fig. 2.16, by interpolation between the contours for $K = 0.2$ and 0.3 to $K = 0.26$, at the appropriate value of d^* in each case. Using the values for ξ and v_{ts} from part (a) gives the results shown in Table 2.3. Note that the variation of ξ over the range of particle sizes is rather small.

Table 2.3. Settling velocity calculations

d (m)	2×10^{-4}	5×10^{-4}	1×10^{-3}	2×10^{-3}
V^* (m/s)	0.0232	0.0367	0.0519	0.0735
Re^*	4.64	18.4	51.9	147
v_{ts}/V^*	1.041	2.105	2.990	3.841
v_{ts} (m/s)	0.0241	0.0772	0.1552	0.2823
d^*	5.05	12.6	25.3	50.5
Ξ	0.55	0.58	0.55	0.52
v_t (m/s)	0.013	0.045	0.085	0.147

REFERENCES

- Clift, R., Grace, J.R. & Weber, M.E. (1978). *Bubbles, Drops and Particles*, Academic Press, New York.
- Grace, J.R. (1986). Contacting modes and behaviour classification of gas-solid and other two-phase suspensions. *Can. J.Chem.Eng.* Vol. 64, pp. 353-363.
- Karassik, I.J., Messina, J.P., Cooper, P. & Heald, C.C.(2001) *Pump Handbook Third Edition*, McGraw- Hill.
- Kay, J.M. & Nedderman, R.M. (1985). *Fluid Mechanics and Transfer Processes*, Cambridge University Press.
- Newton, I. (1726). *Principia Mathematica Philosophiae Naturalis*. 3rd Ed., Book II Scholium to Proposition XL, Royal Society, London. Reprinted by University of Glasgow, 1871. See also *Newton's Principia*, Motte's Translation Revised, Vol. I, University of California Press, Berkeley, CA, 1962.
- Nikuradse, J. (1933). Strömungsgesetze in rauhen Röhren, *Forschungsheft* - Verein deutsche Ingenieure, No. 361.
- Reynolds, A.J. (1974). *Turbulent Flows in Engineering*. Wiley, London.
- Richardson, J.F. & Zaki, W.M. (1954). Sedimentation and fluidisation: Part I. *Trans. Instn. Chem. Engrs.* Vol. 32, pp. 35-53.
- Streeter, V.L., & Wylie, E.B. (1975). *Fluid Mechanics*. McGraw-Hill, New York.
- Turton, R. & Levenspiel, O. (1986). A short note on the drag correlation for spheres. *Powder Technol.* Vol. 47, pp. 83-86.
- Wilson, K.C., Horsley, R.R., Kealy, T., Reizes, J.C. & Horsley, M. (2003). Direct prediction of fall velocities in non-Newtonian materials. *Int'l J. Mineral Proc.*, Vol. 71/1-4 pp. 17-30.
- Wilson, K.C. & Horsley, R.R. (2004). Calculating fall velocities in non-Newtonian (and Newtonian) fluids: a new view. *Proc. Hydrotransport 16*, BHR Group, Cranfield, UK.

<http://www.springer.com/978-0-387-23262-1>

Slurry Transport Using Centrifugal Pumps

Wilson, K.C.; Addie, G.R.; Sellgren, A.; Clift, R.

2006, X, 432 p., Hardcover

ISBN: 978-0-387-23262-1